

Research Paper

# Redox Reaction Investigation of Graphene Nanoribbon

Young-Jun Yu\*

Department of Physics, Chungnam National University, Daejeon 34134, Korea

Received March 19, 2018; revised March 26, 2018; accepted March 27, 2018

**Abstract** The redox reaction on graphene nanoribbon (GNR) field effect transistors(FET) has been studied. In detail, upon employing an electrolyte gating, we verified electron transport performance modulation of GNR FET by monitoring conductance variation under oxidation and reduction processes. The conductance enhancement of GNR via removal of PMMA residue on graphene surface during redox cycles was also observed.

**Keywords:** Graphene, Graphene nanoribbon, Redox, Oxidation, Reduction, Electrolyte

## I. Introduction

Chemical molecular functionalization of carbon based materials, especially oxidation on carbon nanotubes (CNT) and graphene with the aim of tuning the conductance are being strongly emphasized for high performance sensor and switch applications [1-9]. In the case of CNT field effect transistors (FET), oxidation on point defects in one dimensional carbon channels induces conductance variation between insulating and conducting conditions [1,2]. On the other hand, although there has been broad employment of graphene oxide(GO) [5-9] or reduced GO for offering graphene and utilizing for gas sensor, the redox cycle (i.e. cycling between oxidation and reduction) of graphene FET devices has not been clearly studied and understanding of the conductance modulation of two-dimensional carbon channels is still limited. Furthermore, there is an important obstacle to further research in that randomly oxidized positions on carbon networks restraint the regulation of functionalization positions; as such, novel avenues for manipulation of the redox reaction position at nanometer scale should be proposed. Although the realization of non-reversible reduction or oxidation at selective positions of GO or graphene, respectively, revealed by scanning probe microscope, have been reported [10-14], no *in-situ* redox reaction cycle between graphene and GO [15] at nanometer scale in a carbon network area has yet been found.

In this work, it is investigated the redox cycle and doping conditions of graphene nanoribbon (GNR) using a local side gate in a solution electrolyte for understanding the conductance and redox reaction conditions. The conductance

improvement of GNR due to desorption of PMMA residues on graphene surface during redox cycles is also observed.

## II. Experiments

Graphene flakes are prepared by mechanical exfoliation method on Si wafers covered with 280 nm thick SiO<sub>2</sub> and then metal electrodes are contacted by normal e-beam lithography fabrication. Since Ti electrodes naturally form a thin oxide layer in ambient condition, and this oxide layer screens the graphene-electrode contact from electrochemical

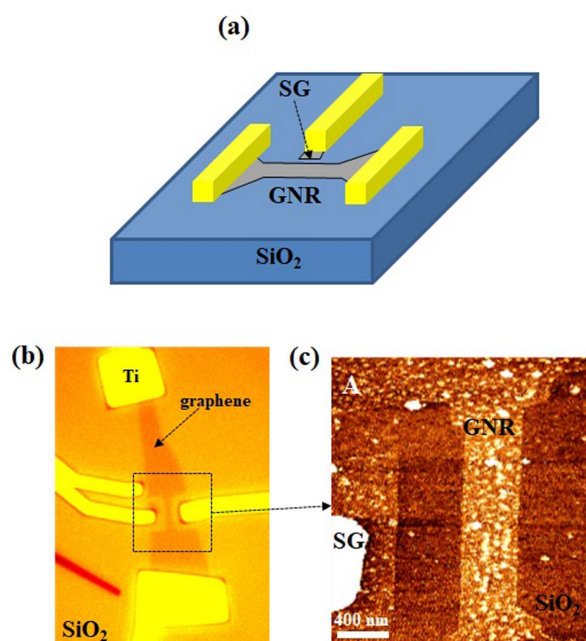


**Figure 1.** (a) Schematic diagram of GNR with side gate (SG). (b) Optical image of GNR. (c) Topographic image of GNR. White dots on GNR indicate PMMA residue.

\*Corresponding author  
E-mail: yjyu@cnu.ac.kr

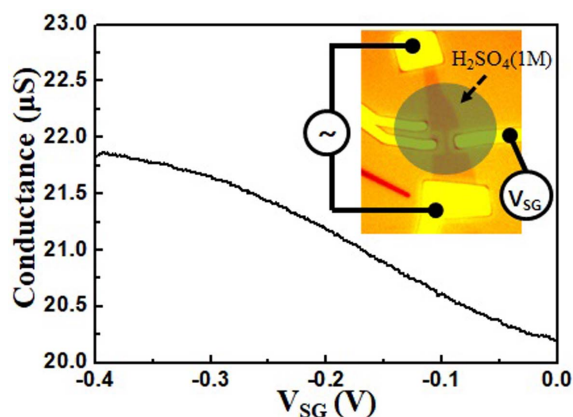


**Figure 2.** Conductance of GNR as a function of  $V_{SG}$  through  $H_2SO_4$  electrolyte. Inset: Optical image of GNR with conductance measurement with  $H_2SO_4$  electrolyte gating circuit schematic diagram.

reaction with the electrolyte, we prepared our samples contacted with Ti electrodes ( $\sim 75$  nm thickness). In order to study the spatially selected redox reaction in a nanometer scale area of graphene, with GNR formed from micrometer scale graphene FETs is used. Figure 1(a) provides a schematic diagram for GNR. This GNR, with channel width  $W = 500$  nm and length  $L = 1$   $\mu m$  (see optical and topographic images in Figure 1(b) and (c)) is prepared by employing a polymethyl methacrylate (PMMA) e-beam resist as an etch mask for an oxygen plasma etching process that removes the unprotected graphene. While the optical microscope image provided in Figure 1(b) does not clearly show the surface condition of the GNR area, the residues on GNR can be observed in the atomic force microscope (AFM, XE-100, Park Systems Corp.) image provided in Figure 1(c). During GNR fabrication, because we employed PMMA as an etch mask for the oxygen plasma etching process, it can be confirmed that the residue on GNR is PMMA.

For the electrochemistry experiment, sulfuric acid ( $H_2SO_4$ , 1M in DI-water) is utilized with simple liquid dropping method on the GNR area, as shown in the inset of Figure 2. As a result, gate voltage can be applied to GNR FET via a side metal electrode with  $H_2SO_4$  electrolyte, the transport curve exhibited values of 20~22  $\mu S$  for  $V_{SG} = -0.4 \sim 0$  V of electrolyte gate voltage range, as shown in Figure 2.

### III. Results and Discussion

Upon applying an  $H_2SO_4$  electrolyte gate voltage larger than  $V_{SG} = -1.7$  V, and because the oxidation on the graphene surface leading to conductance suppression is commenced by the formation of an  $sp^3$  C-O bond, 25% suppression of the conductance to under  $V_{SG} < -1.7$  V was observed, as shown in Figure 3. On the other hand, because the conductance swings back to the initial value of under  $V_{SG} = 0$ , it can be confirmed that the  $sp^3$  C-O bond on the

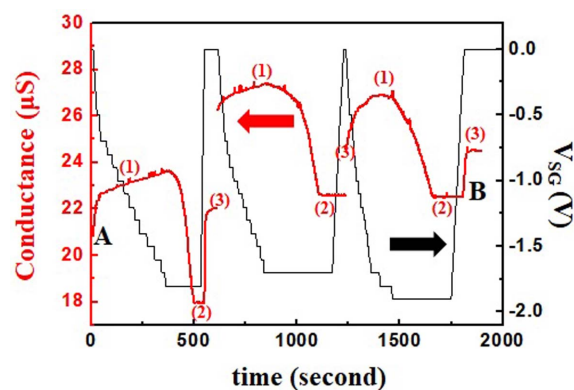


**Figure 3.** (a) Conductance (red line) modulation of SLG induced redox cycle by applied  $V_{EG} = -1.9$  V~0.0 V (black line) in sulfuric acid (1 M). Here A and B indicate the initial and post-initial redox cycle areas. Steps (1), (2) and (3) indicate the conductance variation for the electrolyte gating, oxidation and reduction steps, respectively.

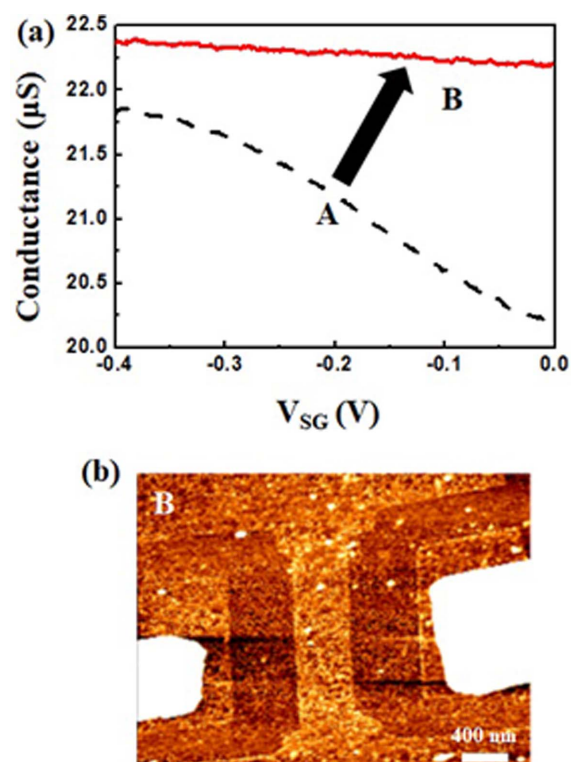


**Figure 4.** (a) Conductance of GNR as a function of  $V_{SG}$  for initial (A) and post-initial (B) redox cycles in Figure 3. Here the conductance line as a function of  $V_{SG}$  (dashed black line) is identical to the data shown in Figure 2(b). (b) Topographic image of GNR after redox cycles in Figure 3.

graphene surface due to  $H_2SO_4$  electrolyte gate voltage is not a permanent condition. As a result, this kind of redox behavior can be continuously observed for the oxidation and reduction steps under  $V_{SG} < -1.7$  V and  $V_{SG} = 0$ , respectively, as shown in Figure 3. The conductance of GNR increases due to the electrolyte gating for application of  $V_{SG} = 0 \sim -1.7$  V (step (1)), and then the conductance of GNR under  $V_{SG} < -1.7$  V is suppressed by oxidation formed C-O or C=O on the GNR surface (step (2)). On

the other hand, under  $V_{SG} = 0$  V, the conductance of GNR is recovered by desorption of oxygen from the oxidized GNR surface (step (3)).

Furthermore, conductance offset exists between the initial condition and the first redox cycle, marked by A and B in Figure 3. A slight conductance enhancement (the highest values from A 21~20  $\mu$ S to B 22  $\mu$ S under  $V_{SG} = -0.4\sim 0$  V) was observed after the first redox cycle. This result can be double-checked by measuring the conductance variation as a function of  $V_{SG}$  which measurement shows the conductance improvement after the first redox cycle, as indicated in Figure 4(a). The origin of the conductance enhancement after the first redox cycle could be the conductance increase of graphene due to increasing accumulated hole carrier density, as well as PMMA residue degradation during the redox cycle. While the transport curve for the initial condition, marked A in Figure 4(a), exhibits conductance suppression in a range from 22  $\mu$ S for  $V_{SG} = -0.4$  to 21  $\mu$ S for  $V_{SG} = 0$  V, which implies that the Fermi level of GNR is approaching a point near the charge neutral position (CNP), transport curve B shows invariant and enhanced types of conductance, which can be ascribed to moving the Fermi level far away from CNP and to desorption of PMMA residue on the graphene surface, respectively. Figure 4(b) provides a topographic image of GNR after the redox cycles shown in Figure 3. Here, compared with the initial topographic image in Figure 1(c), the disappearance of the PMMA residue can be observed. During the redox cycle steps, there is a chemical reaction between PMMA and oxygen under the oxidation step and then this oxidized PMMA can be desorbed from the graphene surface under the reduction step.

#### IV. Summary

This work demonstrates nanometer scale GNR with side gate structure and redox reaction behavior by electrolyte gating. Furthermore, during redox cycles, conductance improvement of GNR was achieved due to desorption of PMMA residue formed during the GNR fabrication

process. This method of removal of polymer residue by redox process can be applied to graphene surface cleaning in various nano-scale graphene structure fabrication processes.

#### Acknowledgements

This work was supported by the research fund of Chungnam National University.

#### References

- [1] E. R. Goldsmith, J. G. Coroneus, V. R. Khalap, A. A. Kane, G. A. Weiss, and P. G. Collins, *Science* 315, 77-81 (2007).
- [2] S. Sorgenfrei, C. Chiu, R. L. Gonzalez, Y. -J. Yu, P. Kim, C. Nuckolls, and K. L. Shepard, *Nature Nanotechnol.* 6, 126-132 (2011).
- [3] X. Wang, X. Li, L. Zhang, Y. Yoon, P. K. Weber, H. Wang, J. Guo, and H. Dai, *Science* 324, 768-771 (2009).
- [4] P. Ramesh, M. E. Itkis, E. Bekyarova, F. Wang, S. Niyogi, X. Chi, C. Berger, W. der Heer, and R. C. Haddon, *J. Am. Chem. Soc.* 132, 14429-14436 (2010).
- [5] G. P. Kotchey, B. L. Allen, H. Vedala, N. Yanamala, A. A. Kapralov, Y. Y. Tyurina, J. Klein-Seetharaman, and V. E. Kagan, *A. Star, ACS Nano* 5, 2098-2108 (2011).
- [6] I. Jung, D. A. Dikin, R. D. Piner, and R. S. Ruoff, *Nano lett.* 8, 4283-4287 (2008).
- [7] L. Liu, S. Ryu, M. R. Tomasik, E. Stolyarova, N. Jung, M. S. Hybertsen, M. L. Steigerwald, L. E. Brus, and G. W. Flynn, *Nano lett.* 8, 1965-1970 (2008).
- [8] A. B. Kalsner, C. Gómez-Navarro, R. S. Sundaram, M. Burghard, and K. Kern, *Nano lett.* 9, 1787-1792 (2009).
- [9] J. T. Robinson, F. K. Perkins, E. S. Snow, Z. Wei, and P. E. Sheehan, *Nano lett.* 8, 3137-3140 (2008).
- [10] L. Weng, L. Zhang, Y. P. Chen, and L. P. Rokhinson, *Appl. Phys. Lett.* 93, 093107 (2008).
- [11] S. Masubuchi, M. Ono, K. Yoshida, K. Hirakawa, and T. Machida, *Appl. Phys. Lett.* 94, 082107 (2009).
- [12] Z. Wei, D. Wang, S. Kim, S.-Y. Kim, Y. Hu, M. K. Yakes, A. R. Laracuente, Z. Dai, S. R. Marder, C. Berger, W. P. King, W. A. der Heer, P. E. Sheehan, and E. Riedo, *Science* 328, 328, 1373-1376 (2010).
- [13] S. Neubeck, L. A. Ponomarev, F. Freitag, A. J. M. Giesbers, U. Zeitler, S. V. Morozov, P. Blake, A. K. Geim, and K. S. Novoselov, *Small* 6, 1469-1473 (2011).
- [14] I. -S. Byun, D. Yoon, J. S. Choi, I. Hwang, D. H. Lee, M. J. Lee, T. Kawai, Y. -W. Son, Q. Jia, H. Cheong, and B. H. Park, *ACS Nano* 5, 6417-6424 (2011).
- [15] Y. Shao, G. Yin, J. Zhang, and Y. Gao, *Electrochem. Acta* 51, 5853-5857 (2006).